Structural and Mechanistic Insight into the Inhibition of Aspartic Proteases by a Slow-Tight Binding Inhibitor from an Extremophilic *Bacillus* sp.: Correlation of the Kinetic Parameters with the Inhibitor Induced Conformational Changes†

Chandravanu Dash, Sangita Phadtare, Vasanti Deshpande, and Mala Rao*

Division of Biochemical Sciences, National Chemical Laboratory, Pune 411 008, India

Received March 23, 2001; Revised Manuscript Received July 13, 2001

ABSTRACT: We present here the first report of a hydrophilic peptidic inhibitor, ATBI, from an extremophilic *Bacillus* sp. exhibiting a two-step inhibition mechanism against the aspartic proteases, pepsin and F-prot from *Aspergillus saitoi*. Kinetic analysis shows that these proteases are competitively inhibited by ATBI. The progress curves are time-dependent and consistent with slow-tight binding inhibition: $E + I \rightleftarrows (k_3, k_4)\ EI \rightleftarrows (k_5, k_6)\ EI^*$. The K_i values for the first reversible complex (EI) of ATBI with pepsin and F-prot were $(17 \pm 0.5) \times 10^{-9}$ M and $(3.2 \pm 0.6) \times 10^{-6}$ M, whereas the overall inhibition constant K_i^* values were $(55 \pm 0.5) \times 10^{-12}$ M and $(5.2 \pm 0.6) \times 10^{-8}$ M, respectively. The rate constant k_5 revealed a faster isomerization of EI for F-prot [$(2.3 \pm 0.4) \times 10^{-3}$ s^{-1}] than pepsin [$(7.7 \pm 0.3) \times 10^{-4}$ s^{-1}]. However, ATBI dissociated from the tight enzyme−inhibitor complex (EI*) of F-prot faster [$(3.8 \pm 0.5) \times 10^{-5}$ s^{-1}] than pepsin [$(2.5 \pm 0.4) \times 10^{-6}$ s^{-1}]. Comparative analysis of the kinetic parameters with pepstatin, the known inhibitor of pepsin, revealed a higher value of k_5/k_6 for ATBI. The binding of the inhibitor with the aspartic proteases and the subsequent conformational changes induced were monitored by exploiting the intrinsic tryptophanyl fluorescence. The rate constants derived from the fluorescence data were in agreement with those obtained from the kinetic analysis; therefore, the induced conformational changes were correlated to the isomerization of EI to EI*. Chemical modification of the Asp or Glu by WRK and Lys residues by TNBS abolished the antiproteolytic activity and revealed the involvement of two carboxyl groups and one amine group of ATBI in the enzymatic inactivation.

The aspartic proteases constitute one of the primary classes of proteolytic enzymes utilizing two aspartic acid residues for their catalytic activity with the direct participation of a lytic water molecule (*1*−*3*). The study of the kinetic properties of this class of enzymes frequently has been motivated by their involvement in physiological and pathological processes of the human. The enzymatic properties of pepsin (the causative agent for peptic ulcer) (*4*), plasma renin (*5*), and lysosomal cathepsin D (*6*), as well as several other aspartic proteases of pharmaceutical and commercial importance (*7*), have evoked considerable interest for investigating the kinetic role of their inhibitors. Recent developments in the involvement of aspartic proteases in the life cycle of human immunodeficiency virus (*8*) and in the degradation of hemoglobin by the malarial parasite (*9*) have generated enormous attention to unravel the interaction between potent inhibitors and the target enzymes.

A number of enzymatic reactions do not respond to the presence of competitive inhibitors instantly but rather display a slow onset of the inhibition. In some cases the inhibitor interacts slowly with the enzyme, and in others the formation of the enzyme−inhibitor complex takes place in a very short time. Such inhibition is called slow-binding inhibition, and the inhibitor is referred to as the slow-binding inhibitor (*10*−*12*). From the kinetic point of view, the possible mechanisms for the slow-binding inhibition phenomena are described in Scheme 1. Scheme 1a assumes that the formation of an EI complex is a single slow step and the magnitude of k_3I is quite small relative to the rate constants for the conversion

Scheme 1[a]

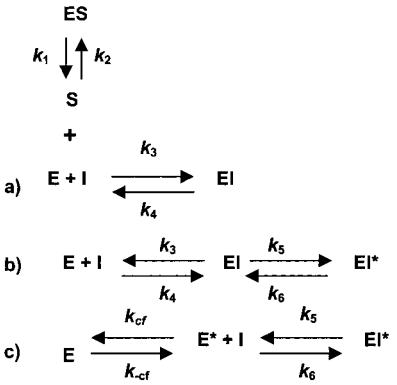

[a] E stands for the free enzyme, I is the free inhibitor, EI is a rapidly forming preequilibrium complex, and EI* is the final enzyme−inhibitor complex. Binding between the enzyme and inhibitor may either involve a single step, having slow association and dissociation rates (Scheme 1a), or have an initial fast binding step, followed by a slow reversible transformation of EI to another entity, EI* (Scheme 1b), or have an initial slow interconversion of the enzyme E into another form, E*, which binds to the inhibitor by a fast step (Scheme 1c).

† C.D. thanks the Council of Scientific and Industrial Research, New Delhi, Government of India, for financial assistance.

* To whom correspondence should be addressed. Telephone: 91-20-589 3034. Fax: 91-20-588 4032. E-mail: malarao@dalton.ncl.res.in.

10.1021/bi010594y CCC: $20.00
Published on Web 08/29/2001

of substrate to product. However, Scheme 1b demonstrates the two-step slow-binding inhibition, where the first step involves the rapid formation of a reversible EI complex, which undergoes slow isomerization to a stable, tightly bound enzyme−inhibitor complex, EI*, in the second step. Inhibitors which inhibit the enzyme-catalyzed reactions at concentrations comparable to that of the enzyme and under conditions where the equilibria are set up rapidly are referred as tight-binding inhibitors. The establishment of the equilibria between enzyme, inhibitor, and enzyme−inhibitor complexes in slow-binding inhibition occurs slowly on the steady-state time scale (*13*), which has been thoroughly reviewed (*14*−*19*). Understanding the basis of the isomerization of the EI complex to the EI* complex could lead to the design of inhibitors that allow titration of the lifetime of the EI* complex. Early investigations of pepsin and the fungal aspartic proteases gave rise to a variety of mechanistic proposals, which were resolved in favor of the mechanisms shown in Scheme 1 (*20*, *21*). The future development of slow-tight binding inhibitors will undoubtedly depend on application of kinetic techniques that yield quantitative information about the properties of the inhibitors.

Considering the physiological importance of the aspartic proteases and their role in various diseases, there is a lacuna in the studies of the mechanism of inhibition by slow-binding inhibitors. To our knowledge, the best-known slow-binding inhibitors of pepsin are pepstatin (*22*) and its analogues (*23*, *24*). However, the hydrophobic nature of pepstatin holds a disadvantage for its poor oral bioavailability. In our earlier report, we have shown that ATBI,[1] with the amino acid sequence of Ala-Gly-Lys-Lys-Asp-Asp-Asp-Asp-Pro-Pro-Glu, exhibited inhibitory activity toward HIV-1 protease (*25*). The present study deals with the evaluation of the kinetic parameters of ATBI, a slow-tight binding inhibitor of the aspartic proteases (AP), pepsin and F-prot from *Aspergillus saitoi*. The fluorescence studies revealed that the binding of ATBI induced localized conformational changes in the proteases, as reflected during the isomerization of the EI complex to the EI* complex. Further, by chemical modification, we have assigned the residues of the inhibitor responsible for the enzyme inactivation.

EXPERIMENTAL PROCEDURES

Bacterial Growth Conditions. The extremophilic *Bacillus* sp. was isolated in this laboratory from the soil sample of a hot spring at Vajreswari, Maharashtra, India (*26*). Biochemical and other tests have indicated its resemblance to *Bacillus pumilus* except for its growth optimum at higher pH and temperature. The optimal growth condition of the *Bacillus* sp. is pH 10 and 50 °C. For the production of the inhibitor the *Bacillus* sp. was grown in a liquid medium containing soyameal (2%) and other nutrients as described (*27*), at 50 °C and pH 10 for 48 h (the pH of the medium was adjusted by the addition of sterile 10% sodium carbonate).

Purification of ATBI. The inhibitor was purified from the extracellular culture filtrate of the *Bacillus* sp. as described previously (*25*). Briefly, about 1000 mL of the extracellular culture filtrate was treated with 65 g of activated charcoal, and the supernatant was subjected to membrane filtration using Amicon UM10 (M_r cutoff 10 000) and UM2 (M_r cutoff 2000). The resulting clear filtrate was concentrated by lyophilization and loaded onto a prepacked Ultopac Lichrosorb RP-18 (LKB) column. The fractions detected at 210 nm were eluted on a linear gradient of 0−50% acetonitrile and water containing 0.01% trifluoroacetate. The active fractions showing the inhibitory activity were pooled and found to be homogeneous by reverse-phase high-performance liquid chromatography.

Enzyme Assays. (a) Pepsin Assay. Pepsin, 75 nM (porcine gastric mucosa), was incubated at 37 °C for 30 min in KCl−HCl buffer, 0.02 M, pH 2.0, with casein (6 mg/mL) or hemoglobin (5 mg/mL) in a reaction volume of 2 mL. The reaction was stopped with an equal volume of 1.7 M perchloric acid (PCA), the mixture was centrifuged (10000*g*, 5 min) and filtered, and the optical absorbance of the filtrate was measured at 280 nm. The enzyme activity was also determined by the Folin−phenol reagent method by estimating the amount of tyrosine released at 660 nm from the standard graph. In the presence of the synthetic substrate *N*-acetyl-L-phenylalanyl-L-3,5-diiodotyrosine, pepsin was assayed as described in ref *28* in an incubation mixture containing a range of substrate concentrations.

(b) Fungal Protease Assay. Proteolytic activity of the purified aspartic protease from *A. saitoi* (F-prot) was measured by assaying the enzyme activity using hemoglobin. F-prot (1.5 μM) was dissolved in glycine−HCl buffer, 0.05 M, pH 3.0, and was incubated with the inhibitor (20 μM) for 5 min. The reaction was started by the addition of 1 mL of hemoglobin (5 mg/mL) at 37 °C for 30 min. The reaction was quenched by the addition of 2 mL of PCA (1.7 M) followed by centrifugation (10000*g*, 5 min) and filtration. The optical absorbance of the PCA-soluble products in the filtrate was read at 280 nm.

For initial kinetic analysis, the kinetic parameters for the substrate hydrolysis were determined by measuring the initial rate of enzymatic activity. The inhibition constant K_i was determined as described by Dixon (*29*) and by the Lineweaver−Burk equation, and the K_m values were calculated from the double reciprocal plots. In Dixon's method, proteolytic activity of the enzymes was measured at two different concentrations of substrate as a function of inhibitor concentration. The kinetic constants were determined by incubating the enzymes in the absence and presence of ATBI with increasing concentrations of the substrate. The inhibition of the initial rate of enzyme activity was analyzed by the double reciprocal plot. One unit of protease activity is defined by an increase of 0.001 at Δ280 nm/min at pH 3.0 at 37 °C measured as PCA-soluble products using hemoglobin/casein as the substrate.

For the progress curve analysis, assays were carried out with 2 mL solutions containing the enzyme, substrate, and inhibitor at various concentrations. Five to six assays were performed in each slow-binding inhibition experiment: one without inhibitor and others with different inhibitor concentrations. At different time intervals, aliquots were removed, and the residual proteolytic activity was measured. Further

[1] Abbreviations: AP, aspartic protease; ATBI, alkalo-thermophilic *Bacillus* inhibitor; AP-ATBI, first reversible aspartic protease−inhibitor complex; AP-ATBI*, second slow dissociating aspartic protease−inhibitor complex; F-prot, fungal protease from *Aspergillus saitoi*; HIV, human immunodeficiency virus; rp-HPLC, reverse-phase high-performance liquid chromatography; CD, circular dichroism; UV, ultraviolet; TNBS, 2,4,6-trinitrobenzenesulfonic acid; WRK, Woodwards reagent K; PCA, perchloric acid.

details of the experiments are given in the respective figure legends. For the kinetic analysis and rate constant determinations, the assays were carried out in triplicate, and the average value was considered throughout this work.

Evaluation of Kinetic Parameters. Initial rate studies that resulted in reversible, competitive inhibition were analyzed according to the equation

$$v = \frac{V_{max}S}{K_m(1 + I/K_i) + S} \quad (1)$$

where K_m is the Michaelis constant, V_{max} is the maximal catalytic rate at saturating substrate concentration [S], K_i is the dissociation constant for the enzyme−inhibitor complex, and I is the inhibitor concentration (*30*).

The progress curves for the interactions between ATBI and aspartic protease as per Scheme 1b were analyzed using the equation (*31*, *32*)

$$[P] = v_s t + \frac{v_0 - v_s}{k}(1 - e^{-kt}) \quad (2)$$

where [P] is the product concentration at any time t, v_0 and v_s are the initial and final steady-state rates, and k is the apparent first-order rate constant for the establishment of the final steady-state equilibrium. For Scheme 1b, the relationship between k, the rate, and the kinetic constants is given by the equation

$$k = k_6 + k_5\left[\frac{I/K_i}{1 + S/K_m + I/K_i}\right] \quad (3)$$

The progress curves were fitted to eqs 2 and 3 using nonlinear least-squares parameter estimation to determine the best fit values.

The overall inhibition constant for Scheme 1b is defined as

$$K_i^* = \frac{[E][I]}{[EI] + [EI^*]} = K_i\left[\frac{k_6}{k_5 + k_6}\right] \quad (4)$$

where $K_i = k_4/k_3$.

For the time-dependent inhibition, there exists a time range in the progress curves in which formation of EI* is small (e.g., see Figure 3). Within this time range, it is possible to directly measure the effect of the inhibitor on v_0, i.e., to measure K_i directly. Values for K_i were obtained from Dixon analysis at a constant substrate concentration (eq 5).

$$\frac{1}{v} = \frac{1}{V_{max}} + \frac{K_m}{V_{max}}(1 + I/K_i) \quad (5)$$

The rate of enzyme−inhibitor dissociation, k_6, was measured directly for the time-dependent inhibition. Small volumes of concentrated enzyme and inhibitor were incubated to reach equilibrium, followed by large dilutions in assay mixtures containing near-saturating substrate. The rate of enzymatic activity regain was measured by the rate of product formation.

Fluorescence Analysis. Fluorescence measurements were performed on a Perkin-Elmer LS50 luminescence spectrometer connected to a Julabo F20 water bath. Protein fluorescence was excited at 295 nm, and the emission was recorded from 300 to 500 nm at 25 °C. The slit widths on both the excitation and emission were set at 5 nm, and the spectra were obtained at 500 nm/min. Fluorescence data were corrected by running control samples of buffer and smoothed.

For inhibitor binding studies, pepsin and F-prot were dissolved in the respective buffer systems. Titration of the enzyme with ATBI was performed by the addition of different concentrations of the inhibitor to the enzyme solution. For each inhibitor concentration on the titration curve a new enzyme solution was used. All of the data on the titration curve were corrected for dilutions. The magnitude of the rapid fluorescence decrease ($F_0 - F$) occurring at each ATBI concentration was computer fitted to the equation $(F_0 - F) = \Delta F_{max}/\{1 + (K_i/[I])\}$ to determine the calculated value of K_i and ΔF_{max}. The first-order rate constants for the slow loss of fluorescence, k_{obs}, at each inhibitor concentration [I] were computer fitted to the equation $k_{obs} = k_5[I]/\{K_i + [I]\}$ for the determination of k_5 under the assumption that, for a tight-binding inhibitor, k_6 can be considered negligible at the onset of the slow loss of fluorescence.

Time courses of the protein fluorescence following the addition of inhibitor were measured for up to 10 min with excitation and emission wavelengths fixed at 295 and 340 nm, respectively. Data points were collected at 0.5 s intervals during time courses. Corrections for the inner filter effect were performed as described by the formula (*33*)

$$F_c = F\ \text{antilog}[(A_{ex} + A_{em})/2]$$

where F_c and F are the corrected and measured fluorescence intensities, respectively, and A_{ex} and A_{em} are the solution absorbances at the excitation and emission wavelengths, respectively. Background buffer spectra were subtracted to remove the contribution from Raman scattering.

Chemical Modification of ATBI with 2,4,6-Trinitrobenzenesulfonic Acid and N-Ethyl-5-phenylisoxazolium-3′-sulfonic Acid. *N*-Ethyl-5-phenylisoxazolium-3′-sulfonic acid (Woodward's reagent K, WRK) has been known to react with the carboxyl group of aspartate and glutamate residues (*34*, *35*). To modify the carboxylic groups, ATBI (50 μM) was incubated in the absence or presence of different concentrations of WRK at 28 °C for 1 h. Aliquots were removed at different time intervals, and the reaction was quenched by the addition of sodium acetate buffer, pH 5.0, to a final concentration of 100 mM. Excess reagent was then removed by gel filtration on a Bio-Gel P2 column, equilibrated with sodium phosphate buffer, 0.05 M, pH 6.0. The fractions were eluted at a flow rate of 12 mL/h. The active fractions were detected by the differential absorption at 210/340 nm and concentrated by lyophilization, and the residual activity of the inhibitor was determined by assaying for the antiproteolytic activity.

ATBI (50 μM) and 0.25 mL of 4% sodium bicarbonate were incubated with varying concentrations of 2,4,6-trinitrobenzenesulfonic acid (TNBS), a lysine group modifier (*36*), at 37 °C in a reaction mixture of 0.5 mL in the dark. Aliquots were withdrawn at suitable intervals, and the reaction was terminated by adjusting the pH to 4.6. A control without the modifier was routinely included, and the residual activity at any given time was calculated relative to the

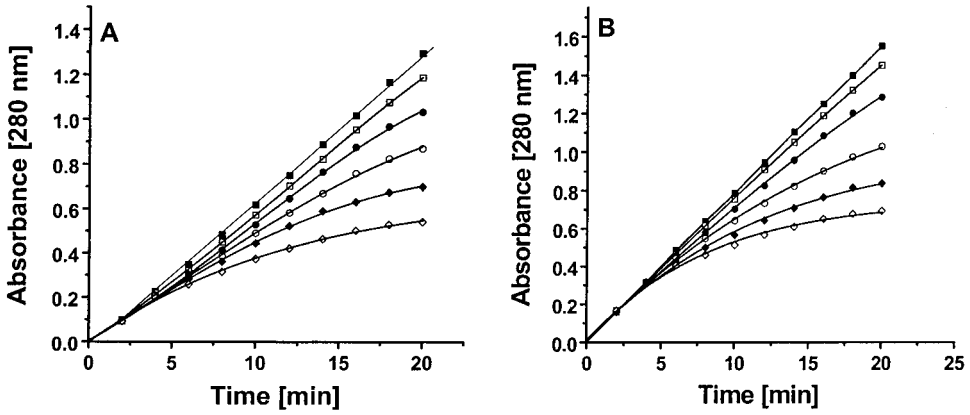

FIGURE 1: Time-dependent inhibition of pepsin and F-prot by ATBI. The reaction solution contained pepsin (50 pM, A) and F-prot (15 nM, B) in respective buffers at increasing concentrations of ATBI using casein (6 mg/mL) or hemoglobin (5 mg/mL). Reactions were initiated by the addition of the enzymes at 37 °C. The points represent the hydrolysis of substrate as a function of time at 37 °C. The lines indicate the best fits of data obtained from eqs 2 and 3. Concentrations of ATBI were 0 nM (■), 10 nM (□), 20 nM (●), 30 nM (○), 40 nM (◆), and 50 nM (◇) in panel A and 0 μM (■), 1 μM (□), 2.5 μM (●), 5 μM (○, 10 μM (◆), and 15 μM (◇) in panel B.

control. The extent of inactivation of pepsin and F-prot was determined with the modified inhibitor as described before.

RESULTS

Kinetic Analysis of the Inhibition of Pepsin and F-prot. ATBI, a peptidic inhibitor of aspartic proteases, was produced extracellularly by an extremophilic *Bacillus* sp. In our earlier report, ATBI was characterized for its anti-HIV-1 protease activity (*25*). Initial kinetic assessments revealed that the aspartic proteases, pepsin and F-prot from *Aspergillus saitoi*, were competitively inhibited by ATBI. Examination of the progress curves suggested that, in the absence of ATBI, the steady-state rate of proteolytic activities was reached rapidly, whereas in its presence, the rate decreased in a time-dependent manner (Figure 1). The progress curves also revealed a time range where the conversion of EI to EI* was minimal. For a low concentration of ATBI, the range was 0−3 and 0−4 min for pepsin and F-prot, respectively, within which classical competitive inhibition experiments can be used to determine the K_i values (eq 3). From such experiments, K_i for ATBI was determined to be $(17 \pm 0.8) \times 10^{-9}$ M for pepsin and $(3.2 \pm 0.5) \times 10^{-6}$ M for F-prot (Figure 2). The K_i associated with the formation of the reversible enzyme−inhibitor complex (AP-ATBI) determined by the Dixon method supported the above values (data not shown). The apparent rate of reaction k from the progress curves when plotted versus the inhibitor concentration followed a hyperbolic function (Figure 3), indicating a two-step inhibition mechanism. Indeed, the data could be fitted to eq 3 by nonlinear regression analysis, which yielded the best estimate of the overall inhibition constant, K_i*, i.e., $(55 \pm 0.5) \times 10^{-12}$ M for pepsin and $(5.2 \pm 0.6) \times 10^{-8}$ M for F-prot.

In an independent method to determine k_6, the rate constant for the conversion of AP-ATBI* to AP-ATBI, high concentrations of enzyme and inhibitor were preincubated for sufficient time to allow the system to reach equilibrium. Further, the enzyme−inhibitor mixture was diluted 10000-fold and assayed at saturating substrate concentration ($100K_m$), which resulted in the dissociation and regeneration of enzymatic activity. Under these conditions, v_0 and the effective inhibitor concentration have been considered to be approximately equal to zero, and the k_6 was determined from the rate of activity regenerated. The values of k_6 determined for pepsin and F-prot were $(2.5 \pm 0.4) \times 10^{-6}$ s^{-1} and $(3.8 \pm 0.5) \times 10^{-5}$ s^{-1}, respectively, by least-squares minimization of eq 2 (Figure 4). The final steady-state rate, v_s, was from the control containing preincubated enzyme without the inhibitor. The half-times, $t_{1/2}$, for reactivation of AP-ATBI* determined from the k_6 values were 77 and 5 h for pepsin and F-prot, respectively. The values of k_5, the rate constant for the isomerization of AP-ATBI to AP-ATBI*, were obtained from fits of eq 3 to the onset of inhibition data, using the experimentally determined values of K_i and k_6 (Table 1).

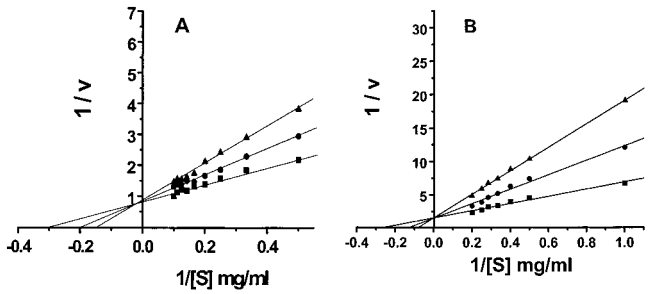

FIGURE 2: Initial rate of reaction in the presence of ATBI. Initial rates of proteolysis by pepsin (A) and F-prot (B) were estimated using casein (6 mg/mL) and hemoglobin (5 mg/mL), respectively. The enzymes were incubated (■) without the inhibitor or with the inhibitor at (●) 15 nM and (▲) 25 nM in panel A and at (●) 5 μM and (▲) 10 μM in panel B and assayed at increasing concentrations of substrate. The reciprocals of the substrate hydrolysis for each inhibitor concentration were plotted against the reciprocals of the substrate concentrations. The straight lines obtained indicated the best fit for the data obtained by nonlinear regression, as analyzed by the Lineweaver−Burk reciprocal equation, and the K_m and K_i values were determined from the graphs. Velocities are in micromoles per minute per milligram.

There are two alternative models for the time-dependent inhibition by Scheme 1 (*31*, *37*). An inhibition model in which the binding of the inhibitor to the enzyme is slow and tight, but occurs in a single step (Scheme 1a), is eliminated on the basis of the data of Table 1, because the inhibitor has a measurable effect on the initial rates before the onset of the slow-tight binding inhibition. An inhibition model where the inhibitor binds only to the free enzyme that has slowly adopted the transition-state configuration (Scheme 1c) can also be eliminated by the observed rates of onset of

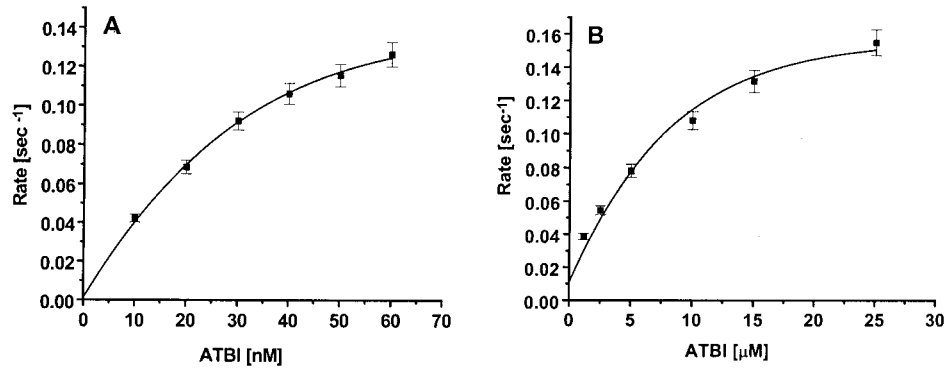

FIGURE 3: Effect of ATBI on the rate of reaction (k) of the proteolytic activity of pepsin and F-prot.The rate constants k were calculated from the progress curves recorded following addition of pepsin (A) or F-prot (B) to the reaction mixture containing the appropriate buffer and substrate. The solid line indicates the best fit of the data obtained.

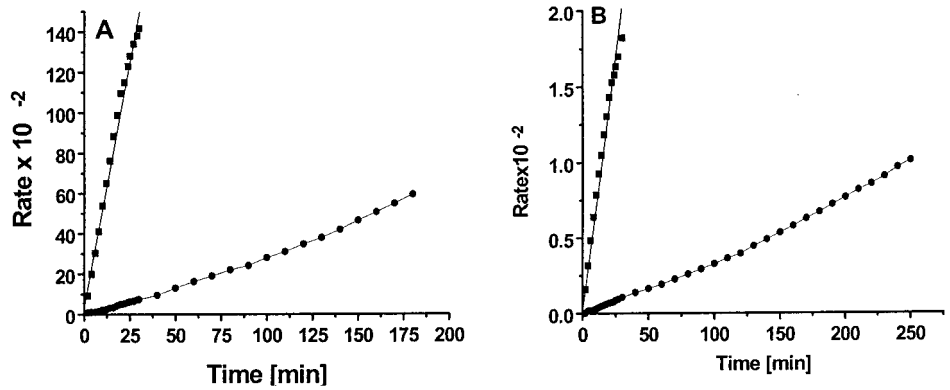

FIGURE 4: Dissociation rate (k_6) for pepsin− and F-prot−ATBI complexes. Pepsin (1 μM, A) and F-prot (100 μM, B) were preincubated without (■) or with (●) equimolar concentrations of ATBI for 120 min on ice in the respective buffered solutions. Further, the enzyme inhibitor mixture was diluted 10 000-fold into the assay mixture containing the substrate at 100K_m (K_m of casein for pepsin, 3.5 mg/mL, and, K_m of Hb for F-prot, 4.3 mg/mL). After preincubation, 2 μL of sample was removed and diluted to 20 mL in the same buffer. At the specified time, aliquots were removed and assayed for the proteolytic activity using casein or hemoglobin. The effective rate (k_6) was determined as described in the text.

Table 1: Inhibition Constants of ATBI and Pepstatin against Pepsin

inhibition constants	inhibitors	
	ATBI[a]	pepstatin[b]
K_i (M)	$17 \pm 0.5 \times 10^{-9}$	1.3×10^{-8}
K_i* (M)	$55 \pm 0.5 \times 10^{-12}$	4.5×10^{-11}
k_5 (s^{-1})	$7.7 \pm 0.3 \times 10^{-4}$	$2.3 \pm 0.4 \times 10^{-3}$
k_6 (s^{-1})	$2.5 \pm 0.4 \times 10^{-6}$	$3.8 \pm 0.5 \times 10^{-5}$
k_5/k_6	310	290
$t_{1/2}$ (h)	77	2.5

[a] The K_i values for competitive inhibition were obtained from the steady-state time range. For the composition of buffers and assay conditions, see Experimental Procedures. [b] Values obtained from Rich et al. (*21*).

inhibition. From the observed results, we have concluded that the inhibition of the aspartic proteases followed the slow-tight binding mechanism as described in Scheme 1b.

Fluorometric Analysis of Enzyme−Inhibitor Interactions. To delineate the conformational changes induced in the aspartic proteases due to the binding of ATBI, the fluorescence spectra of the enzyme−inhibitor complexes were monitored. The tryptophanyl fluorescence spectra of pepsin and F-prot exhibited an emission maxima (λ_{max}) at ~342 nm, as a result of the radiative decay of the $\pi-\pi^*$ transition from the Trp residues (data not shown). The binding of ATBI resulted in a concentration-dependent progressive quenching of the emission spectra of the enzymes. However, λ_{max} of proteases indicated the absence of the blue or red shift in the intrinsic fluorescence, negating any drastic gross conformational changes in the three-dimensional structure of the enzymes. To monitor the isomerization of AP-ATBI to AP-ATBI*, we have followed the intrinsic tryptophanyl fluorescence of the complexes as a function of time. Upon the addition of ATBI, a rapid decrease in the quantum yield of fluorescence was observed, followed by a slow decline to a final stable value over a period of 60 and 25 s for pepsin and F-prot, respectively (Figure 5), indicating an exponential decay of the fluorescence intensity. The magnitude of the rapid fluorescence decrease as a function of time was found to be similar to the total fluorescence quenching observed at a specific ATBI concentration. Thus we have concluded that both AP-ATBI and AP-ATBI* complexes have the same intrinsic fluorescence. Further, titration was performed in which an increased concentration of ATBI was added to the enzymes. The magnitude of the initial rapid fluorescence loss ($F_0 - F$) increased hyperbolically (Figure 6), corroborating the two-step, slow-tight binding inhibition of the aspartic proteases by ATBI. The estimated value of K_i determined by fitting the data for the magnitude of the rapid fluorescence decrease ($F_0 - F$) was $(18.9 \pm 0.5) \times 10^{-9}$ M, and the k_5 value determined from the data derived from the slow decrease in fluorescence was $(8.3 \pm 0.5) \times 10^{-4}$ s^{-1} for pepsin. These rate constants are in good agreement with that obtained from the kinetic analysis of pepsin; therefore, the initial rapid fluorescence decrease can be correlated to the

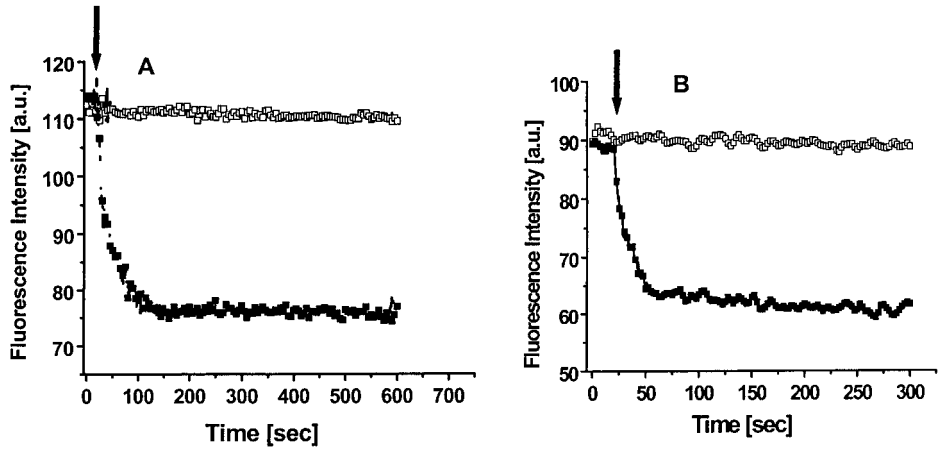

FIGURE 5: Time-dependent effect of ATBI on the fluorescence quenching of the aspartic proteases. Pepsin (100 nM, A) and F-prot (20 μM, B) were treated at the time indicated by the arrows, and the fluorescence emission was followed for 10 min at a data acquisition time of 0.5 s. The excitation wavelength was fixed at 295 nm, whereas the emission wavelength was 342 nm. The data were the average of five scans with the correction for buffer and dilutions. (□) indicates absence of the inhibitor, whereas (■) indicates 35 nM in panel A and 15 μM of ATBI in panel B.

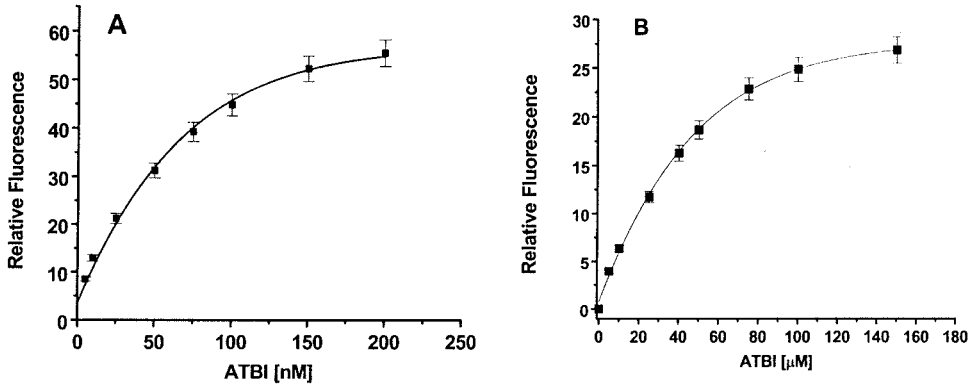

FIGURE 6: Effect of ATBI concentration on the tryptophan fluorescence of the aspartic proteases. A constant amount of pepsin (100 nM, A) and F-prot (20 μM, B) was treated with increasing concentrations of ATBI. The fluorescence changes were measured at 28 °C (excitation, 295 nm, and emission, 342 nm). Each measurement was repeated five times, and the average values of the fluorescence intensity at 342 nm were recorded. Control experiments with the buffer and inhibitor were performed under identical conditions. The fluorescence changes ($F - F_0$) were plotted against the inhibitor concentrations. The hyperbola indicates the best fit of the data obtained.

formation of the reversible complex AP-ATBI, while the slow, time-dependent decrease reflected the accumulation of the tight-bound slow dissociating complex AP-ATBI*.

Chemical Modification of ATBI and Assessment of Its Antiproteolytic Activity. The functional groups involved in the inhibitory activity of ATBI were elucidated by employing chemical modifiers with specific reactivity. The amino acid sequence of ATBI revealed the presence of Lys, Asp, and Glu residues with ionizable side chains. The involvement of these groups in the mechanistic pathway was investigated using WRK, a carboxyl group modifier, and TNBS, an amine group modifier of lysine. Semilogarithmic plots of residual inhibitory activity against the aspartic proteases as a function of time were linear (Supporting Information). The modification of the carboxyl groups of ATBI by WRK was monitored by the differential absorption at 210/340 nm. Analysis of the order of reaction (*38*) for pepsin and F-prot yielded a slope of 1.67 (inset of the Supporting Information) and 1.64 (data not shown), respectively, and thus suggested the involvement of two carboxyl groups in enzyme inactivation. TNBS caused time- and concentration-dependent loss of the inhibitory activity of ATBI. A reaction order of 0.75 (inset of the Supporting Information) and 0.79 (data not shown) for pepsin and F-prot, respectively, determined from the slope of the double logarithmic plot, indicated the involvement of a single amine group of ATBI in the enzyme inactivation.

DISCUSSION

The data presented here showed that ATBI, a peptidic inhibitor from an extremophilic *Bacillus* sp., was a slow-tight binding inhibitor of the aspartic proteases pepsin and F-prot. The determined kinetic data for the enzyme−inhibitor interactions were linked with the conformational changes induced in the enzymes due to the inhibitor binding. During our initial kinetic analysis, the inhibitor showed competitive inhibition against pepsin and F-prot in vitro. The 1:1 molar ratio of the interaction of ATBI with the target enzymes classified it under the "tight-binding inhibitor" group (*39*, *40*). These results were reinforced by the equilibrium binding studies of the enzyme and inhibitor and by the estimation of the residual proteolytic activity.

The slow-binding inhibition of enzymes can be illustrated kinetically by three mechanisms as described in Scheme 1. Simple second-order interaction between the enzyme (E) and the inhibitor (I) could result in slow-binding inhibition where the rate of complex formation is slow. Kinetically, when an inhibitor has a low K_i value and the concentration of *I* varies

in the region of K_i, both k_3I, and k_4 values would be low. These low rates of association and dissociation would lead to slow-binding inhibition (Scheme 1a). Alternatively, binding may also involve two steps where there is a rapid formation of an initial collisional complex, EI, that subsequently undergoes slow isomerization to form the final tight complex EI* (Scheme 1b). The nature of these changes has been discussed (*11*, *41*). The extent of EI* formation depends on the affinity of the EI complex and the relative rates of formation of EI* and its relaxation to EI. Slow-binding inhibitor can also arise due to an initial slow interconversion of the enzyme E into another form E* which binds the inhibitor by a fast step (Scheme 1c). Kinetically, these mechanisms can be differentiated by investigating the behavior of the enzyme−inhibitor system at varying concentrations of the inhibitor. Scheme 1a would predict that in the presence of substrate the initial rate of substrate hydrolysis will be independent of inhibitor concentrations as the concentration of EI would be significantly low. However, in Scheme 1b, the inhibitor will inhibit the enzyme competitively at the onset of the reaction, and at increasing concentration of inhibitor, the initial rate of substrate hydrolysis will decrease hyperbolically. The kinetic properties of the aspartic proteases studied in this report provide a unique opportunity to quantitate these rates and affinities.

As found in most of the ground-state inhibitors, formation of the first reversible complex, AP-ATBI, was too rapid to be measured at steady-state kinetics and was likely to be near diffusion control. The rate of formation of the second enzyme inhibitor complex, AP-ATBI*, was slow and relatively independent of the stability of the AP-ATBI complex or of the ability of the inhibitor to stabilize the AP-ATBI* complex. Thus the major variable for slow-binding inhibition is k_6, the first-order rate at which AP-ATBI* relaxes to AP-ATBI. An equivalent statement is that the apparent inhibitor constant, K_i*, depends on the ability of the inhibitor to stabilize the AP-ATBI* complex. The longer half-life of the AP-ATBI* signified better stability and the slow dissociating nature of these complexes.

It is interesting to comment on the kinetic data of ATBI in the light of the extensive kinetic analysis of pepstatin, the only known tight-binding inhibitor of pepsin. The values of K_i and K_i* for ATBI were observed to be much lower than those of pepstatin. ATBI has a longer half-life and a better k_5/k_6 ratio (the determinant of the kinetic behavior of AP-ATBI*), which clearly indicated the superiority of the ATBI inhibition system to that of pepstatin. However, due to the unavailability of the X-ray crystallographic data of the pepsin−ATBI complex, we are unable to comment on the structural comparison between both the inhibitors. It will be indeed intriguing to compare the X-ray crystallographic data for the identification of the important contacts between the enzyme and the inhibitors, which will facilitate the understanding of the mechanism of inactivation of pepsin by ATBI. With the existing results, ATBI certainly holds an added advantage over pepstatin because of its hydrophilic nature and longer half-life.

The onset of slow-binding inhibition is caused by a normal conformational mode of the enzyme−inhibitor complex that attains the stable configuration. The slow-binding inhibitors combine at the active site and induce conformational changes that cause the enzyme to clamp down in the inhibitor, resulting in the formation of a stable enzyme−inhibitor complex. The time-dependent inhibition kinetics of pepsin and F-prot by ATBI followed a two-step mechanism, which was also reflected in the quenching pattern of the fluorescence. On the basis of our fluorescence studies, we propose that the rapid fluorescence loss was due to the formation of the reversible AP-ATBI complex, whereas the subsequent slower decrease was a result of the accumulation of the tightly bound AP-ATBI* complex. The kinetically observable isomerization of AP-ATBI to AP-ATBI* does not involve a major alteration in the three-dimensional structure of the enzymes as reflected in the absence of any shift in the tryptophanyl fluorescence. Further, agreement of the rate constant values determined from kinetic and fluorescence analysis prompted us to correlate the localized conformational changes to the isomerization of AP-ATBI to AP-ATBI*.

Any changes in the environment of individual tryptophan residues may result in an alternation of fluorescence characteristics such as emission wavelength, quantum yield, and susceptibility to quenching (*42*). Fluorescence quenching can also result from the energy transfer to an acceptor molecule having an overlapping absorption spectrum (*43*). As the inhibitor has no absorption in the region of 290−450 nm, we ruled out the quenching of fluorescence due to the energy transfer between the inhibitor and the tryptophan residues. The possibility that can be considered for the above inhibitor-induced fluorescence decrease is due to the presence of multiple sites, binding at one induced rapid fluorescence change and at a second caused the slow fluorescence decrease. To verify this possibility, a fixed concentration of the enzymes was titrated with increasing concentrations of ATBI. The proteolytic activity of pepsin and F-prot decreased linearly with increasing concentrations of ATBI, yielding a stoichiometry close to 1:1 expected for the slow-tight binding inhibition. The effect of ATBI concentration on the fluorescence quenching of the enzymes was also consistent with a 1:1 molar ratio. These results are therefore inconsistent with the presence of multiple high-affinity sites. Irrespective of the physical explanation for the quenching process, it was apparent that the inhibitor-induced fluorescence quenching followed the formation of both the complexes AP-ATBI to AP-ATBI*.

The amino acids comprising the active center and the correlation between these residues with the inhibitory function are essential to understand the mechanism of action of the inhibitor. Chemical modification and the kinetic analysis indicated the participation of one amine and two carboxyl groups of ATBI in the inhibition of aspartic proteases. The catalytic site of the aspartic proteases consists of two carboxyl groups and an essential lytic water molecule (*44*) and follows a general acid−base catalysis mechanism. The probable explanation for the involvement of two carboxyl groups of ATBI is that they may form a network of hydrogen bonds with the catalytic water molecule and with the ionizable groups in the active site of the enzyme. The participation of the Lys residue may be explained by considering its ability to form hydrogen bonding with the catalytic carboxyl groups of the enzymes. These interactions may interfere in the native weak interactions between the carboxyl groups of the active site and the lytic water molecule, leading toward the inactivation of the enzymes. However, the crystal structure

of the enzyme−inhibitor complex will aid in understanding the mechanism of inactivation of the aspartic proteases in depth.

The results of our investigation demonstrated that the inactivation of pepsin and F-prot by ATBI followed the slow-tight binding inhibition mechanism and can be conveniently monitored by fluorescence spectroscopy. On the basis of our foregoing results, we propose that, concomitant with the kinetic characterization, fluorescence spectroscopy will be useful for the evaluation of inhibitor kinetic constants in the absence of enzyme turnover and for the characterization of the mechanism of inhibition of aspartic proteases by slow-tight binding inhibitors.

ACKNOWLEDGMENT

The authors thank the late Dr. A. M. Bodhe for initial input in this study.

SUPPORTING INFORMATION AVAILABLE

One figure showing the differential labeling of the ionizable groups of ATBI with WRK and TNBS. This material is available free of charge via the Internet at http://pubs.acs.org.

REFERENCES

1. Fruton, J. S. (1976) *Adv. Enzymol. Relat. Areas Mol. Biol. 44*, 1−36.
2. Dunn, B. M. (1992) *Adv. Detailed React. Mech. 2*, 213−241.
3. Davies, D. R. (1990) *Annu. Rev. Biophys. Biophys. Chem. 19*, 189−215.
4. Richardson, C. T. (1985) *Am. J. Med. 79* (Suppl. 2C), 1−7.
5. Thaisrivongs, S. (1989) *Drug News Perspect. 1*, 11−16.
6. Scarborough, P. E., Guruprasad, K., Topham, C., Richo, G. R., Conner, G. E., Blundell, T. L., and Dunn, B. M. (1993) *Protein Sci. 2*, 264−276.
7. Ward, M., and Kodama, K. H. (1991) in *Structure and Function of the Aspartic Proteinases—Genetics, Structure, and Mechanisms* (Dunn, B. M., Ed.) pp 149−160, Plenum Press, New York.
8. Debouck, C., and Metcalf, B. W. (1990) *Drug Dev. Res. 21*, 1−17.
9. Rosenthal, P. J. (1998) *Emerging Infect. Dis. 4*, 49−57.
10. Williams, J. W., and Morrison, J. F. (1979) *Methods Enzymol. 63*, 437−467.
11. Szedlacsek, S., and Duggleby, R. G. (1995) *Methods Enzymol. 249*, 144−180.
12. Sculley, M. J., Morrison, J. F., and Cleland, W. W. (1996) *Biochim. Biophys. Acta 1298*, 78−86.
13. Morrison, J. F. (1982) *Trends Biochem. Sci. 7*, 102−105.
14. Morisson, J. F., and Walsh, C. T. (1988) *Adv. Enzymol. Relat. Areas Mol. Biol. 61*, 201−301.
15. Yiallouros, I., Vassiliou, S., Yiotakis, A., Zwilling, R., Stocker, W., and Dive, V. (1998) *Biochem. J. 331*, 375−379.
16. Ploux, O., Breyne, O., Carillon, S., and Marquet, A. (1999) *Eur. J. Biochem. 259*, 63−70.
17. Merker, D. J., Brenowitz, M., and Schramm, V. L. (1990) *Biochemistry 29*, 8358−8364.
18. Pegg, M. S., and von Itzstein, M. (1994) *Biochem. Mol. Biol. Int. 32*, 851−858.
19. Kati, W. M., Saldivar, A. S., Mohamadi, F., Sham, H. L., Laver, W. G., and Kohlbrenner, W. E. (1998) *Biochem. Biophys. Res. Commun. 244*, 408−413.
20. Suguna, K., Padlan, E. A., Smith, C. W., Catlson, W. D., and Davies, D. R. (1987) *Proc. Natl. Acad. Sci. U.S.A. 84*, 7009−7013.
21. James, M. N. G., Sielecki, A. R., Hayakawa, K., and Gelb, M. H. (1992) *Biochemistry 31*, 3872−3888.
22. Umezawa, H., Takita, T., and Shiba, T., Eds. (1978) *Bioactive Peptides Produced by Microorganisms*, Halsted, New York.
23. Rich, D., and Sun, E. (1980) *Biochem. Pharmacol. 29*, 2205−2212.
24. Gelb, M., Svaren, J., and Abeles, R. (1985) *Biochemistry 24*, 1813−1817.
25. Dash, C., and Rao, M. (2001) *J. Biol. Chem. 276*, 2487−2493.
26. Dey, D., Hinge, J., Shendye, A., and Rao, M. (1991) *Can. J. Microbiol. 38*, 436−442.
27. Dash, C., Phadtare, S. U., Ahmed, A., Deshpande, V. V., and Rao, M. B. (1998) Indian Patent No. 3560-DEL-98.
28. Chiang, L., Sanchez-Chiang, L., Wolf, S., and Tang, J. (1966) *Proc. Soc. Exp. Biol. Med. 122*, 700−710.
29. Dixon, M. (1953) *Biochem. J. 55*, 170−171.
30. Cleland, W. W. (1979) *Methods Enzymol. 63*, 103−138.
31. Beith, J. G. (1995) *Methods Enzymol. 248*, 59−84.
32. Morison, J. F., and Stone, S. R. (1985) *Comments Mol. Cell. Biophys. 2*, 347−368.
33. Lakowicz, J. R. (1983) *Principles of Fluorescence Spectroscopy*, Plenum Press, New York.
34. Arana, J. L., and Vallejos, R. H. (1981) *FEBS Lett. 123*, 103−106.
35. Sinha, U., and Brewer, J. M. (1985) *Anal. Biochem. 151*, 327−333.
36. Okuyama, T., and Satake, K. (1960) *J. Biochem. (Tokyo) 47*, 454−466.
37. Erion, M. D., and Walsh, C. T. (1987) *Biochemistry 26*, 3417−3425.
38. Levy, H. M., Leber, P. D., and Ryan, E. M. (1963) *J. Biol. Chem. 238*, 3654−3659.
39. Williams, J. W., and Morrison, J. F. (1979) *Methods Enzymol. 63*, 437−467.
40. Wolfenden, R. (1976) *Annu. Rev. Biophys. Bioeng. 5*, 271−306.
41. Jencks, W. C. (1975) *Adv. Enzymol. Relat. Areas Mol. Biol. 43*, 219−411.
42. Pawagi, A. B., and Deber, C. M. (1990) *Biochemistry 20*, 950−955.
43. Cheung, H. C. (1991) in *Topics in Fluorescence Spectroscopy, Vol. 2: Principles* (Lakowicz, J. R., Ed.) pp 127−176, Plenum Press, New York.
44. Rao, M. B., Tanksale, A. M., Ghatge, M. S., and Deshpande, V. V. (1998) *Microbiol. Mol. Biol. Rev. 62*, 597−635.

BI010594Y